Volume 10, Issue 4, 2020, 5696 - 5703 ISSN 2069-5837
Biointerface Research in Applied Chemistry
www.BiointerfaceResearch.com
https://doi.org/10.33263/BRIAC104.696703
Original Research Article Open Access Journal
Received: 04.03.2020 / Revised: 25.03.2020 / Accepted: 26.03.2020 / Published on-line: 29.03.2020

Removing skin-cancer damaging based on destroying thymine dimer complexes

Mitra Naeimi [1], Fatemeh Mollaamin [2], Majid Monajjemi [2,*]
[1] Department of biomedical engineering, Central Tehran Branch, Islamic Azad University, Tehran, Iran
[2] Department of chemical engineering, Central Tehran Branch, Islamic Azad University, Tehran, Iran
*corresponding author e-mail address: ***maj.monajjemi@iauctb.ac.ir*** | Scopus ID 6701810683

ABSTRACT
Cyclobutane pyrimidine dimers including thymine or uracil have been studied and characterized through several spectroscopic methods. The azetidin intermediates are generated when the 3'-end bases are cytosine group, through cycloaddition of the 4-imino functional of the latter pyrimidin base. Spontaneous rearrangement of the oxetan or azetidin yields rises to the pyrimidin (6-4) pyrimidon adducts. Chemical shifts, isotropies, anisotropies, spans, asymmetries, and other properties are all the integrals of those current densities that can be explained through magnetic criteria and are the trustworthy accounts of the currents induced via external magnetic field capabilities.
Keywords: *Skin cancer, thymine dimer, NMR shielding.*

1. INTRODUCTION

Thymine-thymine dimerization (T-T) is a problem due to ultraviolet radiation-induced DNA damaging. Human mitochondrial DNA polymerase can be activated the low level translation to synthesize T-T that was further attenuated through exonuclease mechanism. Such damage may inhibit mitochondrial DNA replication and contribute to mutagenesis in vivo. Alterations in mitochondrial, DNA maintenance are associated with skin cancer [1, 2].

Especially in cells have been exposed for moderating, non-cytotoxic levels of UV radiation and carry a significant load of T-T dimers in their DNA that is a likely exposure given the chronic and lifelong nature of sunlight exposure. Due to mitochondria lack nucleotide excision repair needed for repairing T-T dimers, these disruptive lesions will persist in DNA [2, 3]. Systemic or topical application of antioxidants has been suggested as a protective measure against UV-induced skin damage. Skin cancer is very frequent in Caucasians, and its incidence is increasing steadily [4, 5].

This investigated is caused inter alia by demographic changing. Both DNA damage caused via direct absorbance of UV radiation and indirect DNA damage contributed via reactive oxygen species (ROS) may lead to mutations, which can result in UV-induced skin cancer. These two effects within an increased ultraviolet exposure though changes in the recreational phenomenon are the main cause of skin cancer. The exposure to UV radiation promotes the development of squamous cell carcinoma or SCC and its precursor lesions [1-4]. Epidemiologic[6] data also imply UV as a major factor in the etiology of melanoma and basal cell carcinoma or BCC. Two major kinds of thymine dimers generally formed in mammalian cells and unrepaired.

These lesions pose a formidable challenge to cellular DNA replication; indeed, defects in cellular thymine dimer repair machinery have been linked both with human skin cancers and such diseases as "Xeroderma pigmentosum"[6, 7]. As it mentioned UV-induced DNA damage causes an important role in the initiation phase of skin cancer. Due to left unrepaired or damaged cells are not eliminated by apoptosis, DNA lesions express their mutagenic properties. Overexposure to sunlight, and especially to the ultraviolet (UV) portion of its spectrum, is unambiguously linked to the onset of skin cancer as well as photo aging and ocular pathologies.

The main damaging mechanism includes direct absorption of UVB and sometimes UVA photons that trigger dimerization of pyrimidine bases [5-8]. Dimeric photoproducts involving adjacent pyrimidine bases are the most frequent UV-induced lesions in cellular DNA. One of the consequences of these kind formations of excited states is the formation of DNA photo-products [9, 10]. Quickly after UV absorption via DNA, the excitation energies can be delocalized over a few bases into Frenkel excitons as the result of stacking between adjacent bases.

The "World Health Organization" officially recognizes UV rays as an environmental carcinogen and various skin cancers are the most general form of cancer in the world. Melanoma compounds are serious kind of skin cancers that can be found in young adults. Detecting melanoma in its early stages greatly increases the chance of survival and the sun releases three types of ultraviolet radiation (UVA, UVB, and UVC). Among these kind rays, UVA passes entirely through the ozone layer and therefore make up the majority of the UV in the Earth's atmosphere [10-12].

These rays penetrate deeper into skins and are basically responsible for tanning. UVB rays are partially absorbed through the ozone layers. Obviously, UVB rays are responsible for the most sunburns and skin cancers. UVC rays are deadly to humans but fortunately are completely absorbed through the ozone layer. UV will cause a double bond to form between the thymine bases found in the DNA of the skin. A strand of DNA may look something such as C-G-T-C-T-T-C. When the skins are exposed to UV, two thymine molecules will bond together which forms thymine dimer systems [13, 14].

Mutations develop when cell DNA damages are not successfully repaired via natural processes over a period of days. Just as with other types of radiation, increased UV radiation exposure are related to an increased risk for developing cancer [15, 16].

1.2. Melanin photosensitization.

Obviously, melanin has been shown to be involved in UVA induced damages to the DNA of melanoma cells. Electron Spin Resonances can be used for detecting the light-activated melanin in *Xiphophorus* as a function of the incident wavelength between wavelengths of 303 to 436 nm [17].

The figures of this spectrum were completely similar to the action spectrum for melanoma induction. However, the native of the resulting changing in human DNA is not clear due to Xeroderma pigmentosum individuals. Nucleotides excision repairing is thought to work on bulky-types of DNA damaging.

The chemical effects of UVB radiation on DNA are tion at 254 nm. UVB exposures of DNA are known for inducing cyclobutane pyrimidine dimers. Conventional sunscreens absorb UVB and are extensively used for optimizing sunlight induced skin damage. The levels of the range UVB in sunlight are strong function of latitude, whereas UVA is not [18, 19].

The differences between the two types of skins cancer include of the hypothesis that melanomas arise primarily from UVA and visible exposures to melanin, which acts as a photosensitizer to damage the DNA in melanocytes, whereas non-melanomas arise from direct DNA damages arising from the UVB exposures of non-melanin containing cells [20, 21].

Several genes are related to malignant melanoma that among them variants of NRAS and BRAF can be mentioned. About of ~2500 somatic sequences, had non-UVB changes, i.e. no changes at di-pyrimidine sequences, although BRAF was mutant in 55% and NRAS were mutant in 30% of the melanoma cases studied. Presumably, the mutant sequences arose from UVA and visible photosensitized reactions. The chemical reaction of UVB radiation on DNA consists of formation with dimeric photoproducts including two adjacent pyrimidine bases (Fig.1).

Cyclobutane pyrimidine dimers including thymine or uracil have been studied and characterized through several spectroscopic methods [22]. The azetidin intermediates are generated when the 3'-end bases are cytosine group, through cycloaddition of the 4-imino functional of the latter pyrimidin base. Spontaneous rearrangement of the oxetan or azetidin yields rises to the pyrimidin (6-4) pyrimidon adducts (Fig. 2).

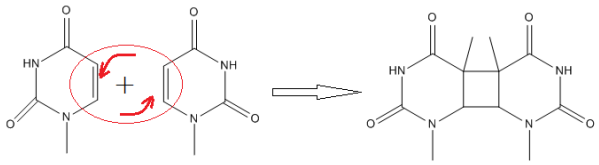

Figure 1. Formation of thymine cyclobutane dimers

The peculiar photo chemical physic features of the lesions are mainly accounted for by the presence of a substituted pyrimidon ring. The latter moiety exhibits fluorescence properties, with excitation and emission maxima around 320 and 380 nm, respectively. The TT, TC and CT photoproducts, as well as their Dewar valence isomers, have been isolated and characterized. In cyclobutane pyrimidine dimers, the pyrimidines, as a consequence of the cyclobutane ring between C5-C5 and C6-C6 of adjacent pyrimidines, have lost their aromaticity and no longer absorb the UV component of sunlight (around 300 nm) and thus are not subject to direct photo reversal in nature. Moreover, the loss of aromaticity also makes the dimers resistant to non-enzymatic degradation by extreme heat or pH that they may encounter in nature.

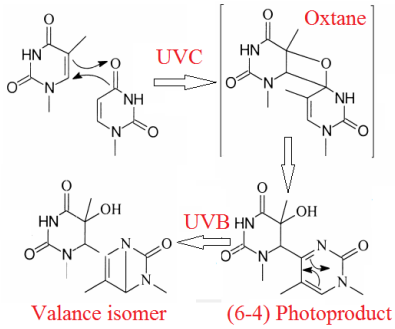

Figure 2. Formation and photo isomerization of the thymine (6-4) photo product

2. MATERIALS AND METHODS

2.1. Isotropic and anisotropic parameters.

The total chemical shielding tensor σ is a non-symmetric tensor which can be separated into three independent parameters: anisotropic, traceless symmetric and traceless anti-symmetric. The spherical tensor has been exhibited by Haeberlen and Mehring. They have investigated fundamental tensors as $\zeta_{zz} = (\sigma_{zz} - \sigma_{iso}) = (\sigma_{33} - \sigma_{iso})$

Where ζ_{zz} is the reduced anisotropy and can be calculated through: the asymmetry shielding (η) can be calculated as: $= \left(\frac{\sigma_{yy}-\sigma_{xx}}{\zeta_{zz}}\right)$. It is notable that the spin magnetic resonance is seldom isotropic, therefore they have to be represented by new tensors (Herzfeld—Berger notation). These tensors are known as span (Ω), which describe the maximum width of the model and the skew (K) of the tensor being $\Omega = \sigma_{33} - \sigma_{11}$. Moreover, the asymmetry tensor orientation is given by: $K = \frac{3(\sigma_{iso}-\sigma_{22})}{\Omega}$

$(-1 \leq K \leq +1)$ in some cases of an axially symmetric tensor, $((-1 \leq \eta \leq +1)$ will be zero, and hence, $\eta = 0$. However, the asymmetry (η) indicates how great deviation can appear from an axially symmetric tensor, therefore the region is $-1 \leq \eta \leq +1$.

2.2. Aromaticity.

Chemical shifts, isotropies, anisotropies, spans, asymmetries, and other properties are all the integrals of those current densities that can be explained through magnetic criteria and are the trustworthy accounts of the currents induced via external magnetic field capabilities. As for the magnetic criterion, the resultant of all such components explains the aromaticity or antiaromaticity, those are related to the net diatropicity & paratropicity of the ring current respectively. Aromaticity and antiaromaticity are conjugation or hyper-conjugation which produces closed two- and three-dimensional electronic circuits. Conjugation, hyper-conjugation, and aromaticity lead for stabilizing interactions which influence the geometries, electron densities, dissociation energies or nuclear magnetic resonance properties among many other physical chemical observables. Despite their importance and widespread apply, neither hyper-conjugation nor aromaticity has a strict physical definition and,

consequently, these properties cannot be experimentally directly measured. These two properties share the same origins which are stabilization due to electron delocalization. Indeed, differences between these two concepts are minor as compared to similarities.

Thus, the claim that one property is more rigorous than the other is totally unfounded.

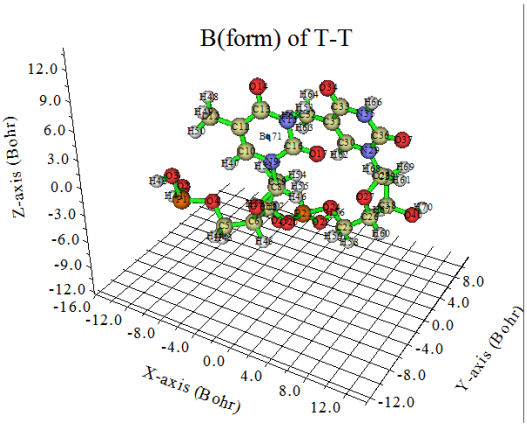

Figure 3. Thymine dimer structure in B forms conformation.

Aromaticity is one of the most major phenomena widely applied in modern chemistry. Its multidimensional composite character lies at the basis of this situation. Since aromaticity is not only peculiar to organic chemical species but also inorganic chemical species, it has a broad area of usage in almost all disciplines of chemistry. The structure of the thymine dimer lesion in DNA oligonucleotide duplexes has been studied both by nuclear magnetic resonance (NMR) and X-ray crystallographic methods and compared to normal B-form DNA duplexes. In the crystal shape, the thymine dimers are somewhat distorted, but the main of the distortion is localized to the immediate vicinities of the dimer with the rest of the DNA B-form conformation (Fig.3). Despite its unusual configuration and loss of the aromaticity, thymine dimers are buried within the right-handed helixes with their neighbors, and paired with their complementary adenines in a manner reasonably similar to normal thymine. However, the duplexes are subtly strained to accommodate the constrained thymine dinucleotide: the phosphate backbones are pinched, both grooves are widened, the base pairing among the 5′ thymine and its adenine pairs are significantly weakened. Therefore the base pair on the 5′ side of the lesion has unusual tilt and twist angles as compared to canonical B-form DNA. These changing angles in DNA duplex to be bent via ~30° toward the main groove and unwound via about 9° in the vicinities of the lesion.

Delocalization and resonance are among the most powerful and widely used concepts in organic chemistry. For many years organic chemists have assumed, often without the support of experimental data, that any planar conjugated π-system that can be represented by a delocalized structure, and hence might be capable of resonance, must indeed become delocalized and hence stabilized (or destabilized) by resonance. Thus, organic chemists have assumed that all molecules that possess the characteristics that should enable them to obey Hückel's Rules for aromaticity, must indeed, in their ground states, be truly delocalized, be resonance stabilized, and hence be aromatic. This assumption has become a "rule" that can only be tempered by the existence of structural or stereo chemical factors that would prevent delocalization, or if the accompanying energetic consequences of delocalization would obviously and undoubtedly be severely unfavorable. Theoretical and computational treatments of conjugated π-systems have also allowed us to ignore instances in which molecules disobey the hallowed rules of delocalization, resonance and aromaticity. The popular molecular orbital theoretical methods allow bonding interactions over very large distances, much greater than those bonds of the same types whose parameters have been determined from the diffraction studies. For example, while there are no instances in which an isolated C=C (carbon–carbon double) bond has ever been shown by experimental diffraction methods to exceed 1.4 Å in length, we often see π-like bonding interactions being invoked in theoretical simulations over distances that are often considerably longer than 1.53 Å, the length of a simple isolated C–C (carbon–carbon) single bond.

2.3. Energy density of thymine rings.

Densities of electron localization and chemical reactivity respectively have been investigated by Bader [28]. The electron densities of hetero rings have been defined as equation in follows;

$(r) = \eta_i \left|\varphi_i(r)\right|^2 = \sum_i \eta_i \left|\sum_l C_{l,i}\,\chi_i(r)\right|^2$ (14). $\rho(r) = [(\frac{\partial\rho(r)}{\partial(x)})^2 + (\frac{\partial\rho(r)}{\partial(y)})^2 + (\frac{\partial\rho(r)}{\partial(z)})^2]^{\frac{1}{2}}$ (15) $\nabla^2\rho(r) = \frac{\partial^2\rho(r)}{\partial x^2} + \frac{\partial^2\rho(r)}{\partial y^2} + \frac{\partial^2\rho(r)}{\partial z^2}$. The density of kinetic energies is not uniquely defined, since the value of kinetic energies operators $< \varphi \left| -\left(\frac{1}{2}\right)\nabla^2 \right| \varphi >$ recovered via integrating densities kinetic energies definition. One of a basic explanation is: $k(r) = -\frac{1}{2}\sum_i \eta_i \varphi_i^*(r)\nabla^2\varphi_i(r)$ "G(r)" is also known as positive definite kinetic energies densities as follows

$G(r) = \frac{1}{2}\sum_i \eta_i \left|\nabla(\varphi_i)\right|^2 =$

$\frac{1}{2}\sum_i \eta_i\{[(\frac{\partial\varphi_i(r)}{\partial(x)})^2 + (\frac{\partial\varphi_i(r)}{\partial(y)})^2 + (\frac{\partial\varphi_i(r)}{\partial(z)})^2]\}$. K(r) and G(r) are straightly related to Laplacian of electron densities $\frac{1}{4}\nabla^2\rho(r) = G(r) - K(r)$ .Becke and Edgecombe explained about the Fermi hole for suggesting electron localization functions (ELF).

ELF(r) $= \frac{1}{1+[D(r)/D_{0(r)}]^2}$ where D(r) $= \frac{1}{2}\sum_i \eta_i \left|\nabla\varphi_i\right|^2 - \frac{1}{8}[\frac{\left|\nabla\rho_\alpha\right|^2}{\rho_\alpha(r)} + \frac{\left|\nabla\rho_\beta\right|^2}{\beta(r)}]$ and $D_{0(r)} = \frac{3}{10}(6\pi^2)^{\frac{2}{3}}[\rho_\alpha(r)^{\frac{5}{3}} + \rho_\beta(r)^{\frac{5}{3}}]$ (23) for close-shell system, since $\rho_\alpha(r) = \rho_\beta(r) = \frac{1}{2}\rho$, D and $D0$ terms can be simplified as D(r) $= \frac{1}{2}\sum_i \eta_i \left|\nabla\varphi_i\right|^2 - \frac{1}{8}[\frac{\left|\nabla\rho\right|^2}{\rho(r)}]$, $D_{0(r)} = \frac{3}{10}(3\pi^2)^{\frac{2}{3}}\rho(r)^{\frac{5}{3}}$, Savin *et al.* have reinterpreted the ELF in the view point of kinetic energies, which makes ELF also explaining for Kohn-Sham DFT wave-function. They exhibited D(r) reveals the excess densities of kinetic energies caused by Pauli repulsion, while D_0 can be considered as Thomas-Fermi densities of kinetic energies. Localized orbital locator (LOL) is another function for locating high localization regions likewise ELF, defined by Chmider and Becke in the paper. $LOL(r) = \frac{\tau(r)}{1+\tau(r)}$ (26), Where, $(r) = \frac{D_0(r)}{\frac{1}{2}\sum_i \eta_i \left|\nabla\varphi_i\right|^2}$ (Lu, T, 2012).

We have simulated our system based on our previous work [24-79].

3. RESULTS

The comparison between thymine dimers yield in nucleic acids with A-form, B-form and Z -type double helical structures help the hypothesis that dimerization in double-stranded DNA appears due to uncommon conformations (Fig.4) [80].

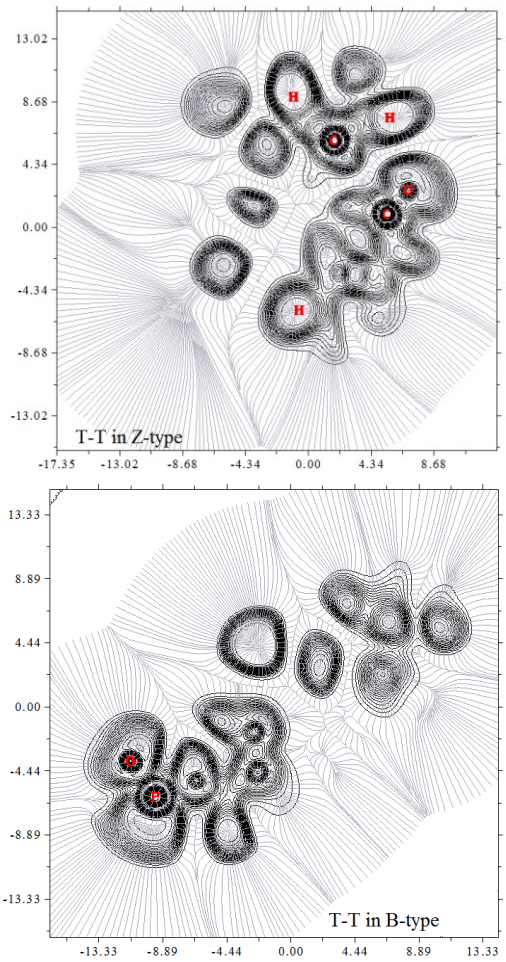

Figure 4. ELF of electron density in two forms conformation Of thymine –thymine dimerization [80]

Rating of dimer formations is decreased to a factor of two when double-stranded DNAs are switched from B-form to A-form conformation. The larger protective effect has been seen at T-T steps in hairpins with A-form conformation. Same bases pairing are found in both structural conformations, and the differences are only the distribution of accessible structural conformations. This establishing can control reactivity in duplex DNA just as in single-stranded. The average twist angles among successive base pair refer in A-DNA via only a few degrees compared to B-DNA, suggesting that ideal geometries in both helices are nonreactive. Although dimerization to take place at T-T steps deviate from the average duplex structure, the smaller amount of conformational appear in A-form vs. B-form structures (Fig.5).

Although base pairing potentially, affects the rates of non-reactivity decay steps like internal conversions through the precursor excited states, considering this unlikely as recent time-resolved measurements exhibit no effects due to base pairing on the dynamics of excited states in A-T bas paring. We calculated that dimerization appears with equal speed for bi-pyrimidine doublets in single- and double-stranded contexts providing that the thymine-thymine geometries are similar. A flexible structure of thymine oligomers and double-stranded mixed-sequences differ significantly this means that the small percentages of T-T dimers react in double stranded DNA even though virtually all are well stacked. The NMR data for thymine is shown in Fig.6.

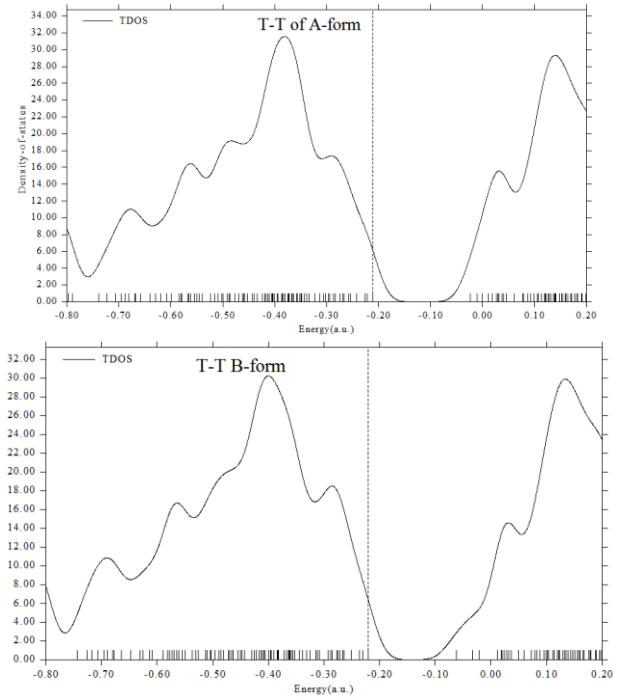

Figure 5. Density of states of T-T forms (A & B).

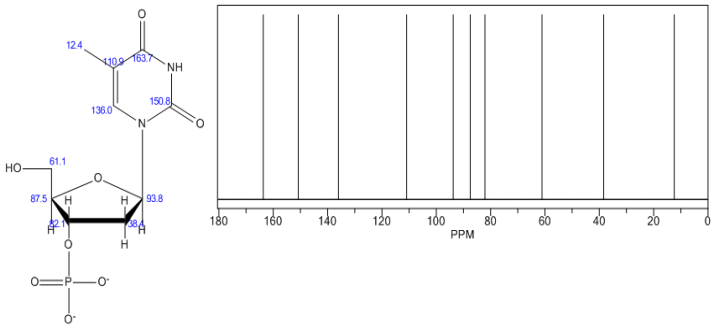

Figure 6. C-NMR data of thymine.

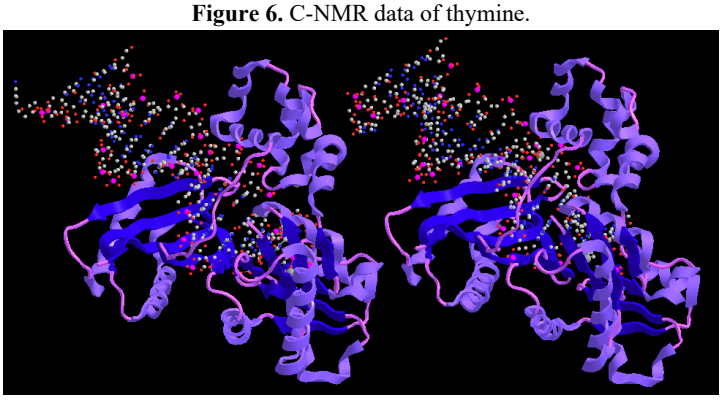

Figure 7. Replication of a cis-syn thymine dimer at atomic resolution.

The winding of base pairs around the helix axis with a twist angle is 35.5° in B-DNA, while C5=C6 is double bonds. In contrast, although in single-stranded thymine oligomers are rare, the more flexible backbones do not prevent those rare from adopting conformation for dimerization perfectly. Due to the rate of reaction via favorably aligned thymine is much quicker than the rate of conformational change. A few percentages of T-T dimers

are favorably positioned for reaction at the time of excitation. The ultrafast scales of thymine duplication suggest which an essential barrier is needed for initial 1ππ* states with the end product which means a conical intersection lies along this path as in computational studies of other pericyclic photoreactions. In Fig.7, Crystal Structure of a DNA r containing a thymine-dimer can be seen.

These dimers are awkward and form a stiff kink in the DNA. This causes problems when the cell needs to replicate its DNA. DNA polymerase has trouble reading the dimer, since it doesn't fit smoothly in the active site. T-T dimers like the ones shown here is not the major problem, since they are usually paired correctly with adenine when the DNA is replicated. But C-C dimers do not fare as well. DNA polymerase often incorrectly pairs adenine with them instead of guanine, causing a mutation. If this happens to be in an important gene that controls the growth of cells, such as the genes for p53 tumor suppressor, the mutation can lead to cancer.

4. CONCLUSIONS

Rating of dimer formations is decreased to a factor of two when double-stranded DNAs are switched from B-form to A-form conformation. Due to the rate of reaction via favorably aligned thymine is much quicker than the rate of conformational change. A few percentages of T-T dimers are favorably positioned for reaction at the time of excitation. An understanding of the effects of sunlight on human skin begins with the effects on DNA and extends to cells, animals and humans. The major DNA photoproducts arising from UVB (280-320 nm) exposures are cyclobutane pyrimidine dimers. If unrepaired, they may kill or mutate cells and result in basal- and squamous cell carcinomas. Delocalization and resonance are among the most powerful and widely used concepts in organic chemistry. For many years organic chemists have assumed, often without the support of experimental data, that any planar conjugated π-system that can be represented by a delocalized structure, and hence might be capable of resonance, must indeed become delocalized and hence stabilized (or destabilized) by resonance.

5. REFERENCES

1. Coroneo, M.T.; Müller-Stolzenburg, N.W.; Ho, A. Peripheral light focusing by the anterior eye and the ophthalmohelioses. *Ophthalmic Surg*. **1991**, *22,* 705-11.
2. Lucas, R.M.; Repacholi, M.H.; McMichael, A.J. Is the current public health message on UV exposure correct? *Bull World Health rgan*. **2006**, *84*, 485-91, https://doi.org/10.2471/blt.05.026559.
3. Oliva, M.S.; Taylor, H. Ultraviolet radiation and the eye. *Int Ophthalmol Clin*. **2005**, *45*, 1-17
4. Schreier, W.J.; Schrader, T.E.; Koller, F.O. Tymine dimerization in DNA is an ultrafast photoreaction. *Science* **2007**, *315,* 625-9, https://doi.org/10.1126/science.1135428.
5. MacLaughlin, J.A.; Anderson, R.R.; Holick, M.F. Spectral character of sunlight modulates photosynthesis of previtamin D3 and its photoisomers in human skin. *Science* **1982**, *216*, 1001-3, https://doi.org/10.1126/science.6281884.
6. Holick, M.F.; Chen, T.C. Vitamin D defciency: a worldwide problem with health consequences. *Am J Clin Nutr*. **2008**, *87,* 1080S-6S, https://doi.org/10.1093/ajcn/87.4.1080S.
7. Wolpowitz, D.; Gilchrest, B.A. Te vitamin D questions: how much do you need and how should you get it? *J Am Acad Dermatol*. **2006**, *54*, 301-17, https://doi.org/10.1016/j.jaad.2005.11.1057.
8. Rosen, E.S. Filtration of non-ionizing radiation by the ocular media. In: *Hazards of Light: Myths and Realities of Eye and Skin. Oxford: Pergamon Press.* Cronly-Dillon, J.; Rosen, E.S.; Marshall, J. eds.1986; pp. 145-52.
9. Walsh, J.E.; Bergmanson, J.P.G.; Koehler, L.V. Fibre optic spectrophotometry for the in vitro evaluation of ultraviolet radiation (UVR) spectral transmittance of rabbit corneas. *Physiological Measurement* **2008**, *29,* 375-88.
10. Kolozsvári, L.; Nógrádi, A.; Hopp, B.; UV absorbance of the human cornea in the 240- to 400-nm range. *Invest Ophthalmol Vis Sci*. **2002**, *43,* 2165-8.
11. Anders, F.; Schartl, M.; Barnekow, A.; Anders, A. *Xiphophorus* as an *in vivo* model for studies on normal and defective control of oncogenes. *Adv Cancer Res* **1984**, *42*, 191-275, https://doi.org/10.1016/s0065-230x(08)60459-5.
12. Setlow, R.B.; Woodhead, A.D.; Grist, E. Animal model for ultraviolet radiation-induced melanoma: Platyfish-swordtail hybrid. *Proc Natl Acad Sci* **1989**, *86,* 8922-8926, https://dx.doi.org/10.1073%2Fpnas.86.22.8922.
13. Setlow, R.B.; Grist, E.; Thompson, K.; Woodhead, A.D. Wavelengths effective in induction of malignant melanoma. *Proc Natl Acad Sci* **1993**, *90,* 6666-6670, https://doi.org/10.1073/pnas.90.14.6666.
14. Setlow, R.B. Spectral regions contributing to melanoma: personal view. *J Invest Dermatol Symp Proceeding* **1999**, *4*, 46-49, https://doi.org/10.1038/sj.jidsp.5640180.
15. Wood, S.R.; Berwick, M.; Ley, R.D.; Walter, R.B.; Setlow, R.B.; Timmins, G.S. UV causation of melanoma in *Xiphophorus* is dominated by melanin photosensitized oxidant production. *Proc Natl Acad Sci* **2006**, *103,* 4111-4115, https://doi.org/10.1073/pnas.0511248103.
16. Kraemer, K.H.; Lee, M.M.; Andrews, A.D.; Lambert, W.C. The role of sunlight and DNA repair in melanoma and nonmelanoma skin cancer. *Arch Dermatol* **1994**, *130,* 1018-1021.
17. Diffey, D.L.; Healy, E.; Thody, A.J.; Rees, J.L. Melanin, melanocytes, and melanoma. *The Lancet* **1995**, *346,* 1713, https://doi.org/10.1016/s0140-6736(95)92882-0.
18. Magnus, K. The Nordic profile of skin cancer incidence. A comparative epidemiological study of the three main types of skin cancer. *Int J Cancer* **1991**, *47,* 12-19, https://doi.org/10.1002/ijc.2910470104.
19. Moan, J.; Dahlback, A.; Setlow, R.B. Epidemiological support for an hypothesis for melanoma induction indicating a role for UVA radiation. *Photochem Photobiol* **1999**, *70*, 243-247, https://doi.org/10.1111/j.1751-1097.1999.tb07995.x.
20. Autier, P.; Dore,' J.F.; Schifflers, E.; Cesarini, J.P.; Bollaerts, A.; Koelmel, K.F.; Gefeller, O.; Liabeuf, A.; Lejune, F.; Lienard, D.; Joarelette, M.; Chemaly, P.; Kleeberg, U.R. Melanoma and use of sunscreens: An EORTC case-control study in Germany, Belgium and France. *Int J Cancer* **1995**, *61,* 749-755, https://doi.org/10.1002/ijc.2910610602.
21. Diffey, B.L. Sunscreens and melanoma:the future looks bright. *British J Dermatol* **2005**, *153,* 378-381, https://doi.org/10.1111/j.1365-2133.2005.06729.x.
22. Gallagher, R.P.; Spinelli, J.J.; Lee, T.K. Tanning beds, sunlamps, and risk of cutaneous malignant melanoma. *Cancer*

Epidemiol Biomarkers Prev **2005**, *14,* 562-566, https://doi.org/10.1158/1055-9965.EPI-04-0564.
23. Hocker, T.; Tsao, H. Ultraviolet radiation and melanoma: A systematic review and analysis of reported sequence variants. *Human Mutation* **2007**, *28,* 578-588, https://doi.org/10.1002/humu.20481.
24. Mollaamin, F.; Monajjemi, M.; Mehrzad, J. Molecular Modeling Investigation of an Anti-cancer Agent Joint to SWCNT Using Theoretical Methods. *Fullerenes nanotubes and carbon nanostructures* **2014**, *22*, 738-751, https://doi.org/10.1080/1536383X.2012.731582.
25. Mollamine, F.; Monajjemi, M. DFT outlook of solvent effect on function of nano bioorganic drugs. *Physics and Chemistry of Liquids* **2012**, *50*, 596-604, https://doi.org/10.1080/00319104.2011.646444.
26. Mollaamin, F.; Gharibe, S.; Monajjemi, M. Synthesis of various nano and micro ZnSe morphologies by using hydrothermal method. *International Journal of Physical Sciences* **2011**, *6*, 1496-1500.
27. Monajjemi, M. Graphene/(h-BN)*n*/X-doped raphene as anode material in lithium ion batteries (X = Li, Be, B AND N). *Macedonian Journal of Chemistry and Chemical Engineering* **2017**, *36*, 101–118, http://dx.doi.org/10.20450/mjcce.2017.1134.
28. Monajjemi, M. Cell membrane causes the lipid bilayers to behave as variable capacitors: A resonance with self-induction of helical proteins. *Biophysical Chemistry* **2015**, *207*, 114-127, https://doi.org/10.1016/j.bpc.2015.10.003.
29. Monajjemi, M. Study of CD5+ Ions and Deuterated Variants (CHxD(5-x)+): An Artefactual Rotation. *Russian Journal of Physical Chemistry A* **2018,** *92***,** 2215-2226.
30. Monajjemi, M. Liquid-phase exfoliation (LPE) of graphite towards graphene: An ab initio study. *Journal of Molecular Liquids*, **2017**, *230*, 461–472, https://doi.org/10.1016/j.molliq.2017.01.044.
31. Jalilian, H.; Monajjemi, M. Capacitor simulation including of X-doped graphene (X = Li, Be, B) as two electrodes and (h-BN)m (m = 1–4) as the insulator. *Japanese Journal of Applied Physics* **2015**, *54,* 085101-7.
32. Ardalan, T.; Ardalan, P.; Monajjemi, M. Nano theoretical study of a C 16 cluster as a novel material for vitamin C carrier. *Fullerenes Nanotubes and Carbon Nanostructures* **2014**, *22*, 687-708, https://doi.org/10.1080/1536383X.2012.717561.
33. Mahdavian, L.; Monajjemi, M.; Mangkorntong, N. Sensor response to alcohol and chemical mechanism of carbon nanotube gas sensors. *Fullerenes Nanotubes and Carbon Nanostructures* **2009***, 17*, 484-495, https://doi.org/10.1080/15363830903130044.
34. Monajjemi, M.; Najafpour, J. Charge density discrepancy between NBO and QTAIM in single-wall armchair carbon nanotubes. *Fullerenes Nanotubes and Carbon Nano structures* **2014**, *22*, 575-594, https://doi.org/10.1080/1536383X.2012.702161.
35. Monajjemi, M.; Hosseini, M.S. Non bonded interaction of B16 N16 nano ring with copper cations in point of crystal fields. *Journal of Computational and Theoretical Nanoscience* **2013**, *10*, 2473- 2477
36. Monajjemi, M.; Mahdavian, L.; Mollaamin, F. Characterization of nanocrystalline silicon germanium film and nanotube in adsorption gas by Monte Carlo and Langevin dynamic simulation. *Bulletin of the Chemical Society of Ethiopia* **2008**, *22*, 277-286, https://doi.org/10.4314/bcse.v22i2.61299.
37. Lee, V.S.; Nimmanpipug, P.; Mollaamin, F.; Thanasanvorakun, S.; Monajjemi, M. Investigation of single wall carbon nanotubes electrical properties and normal mode analysis: Dielectric effects. *Russian Journal of Physical Chemistry A,* **2009**, *83*, 2288-2296, https://doi.org/10.1134/S0036024409130184.
38. Mollaamin, F.; Najafpour, J.; Ghadami, S.; Akrami, M.S.; Monajjemi, M. The electromagnetic feature of B N H (x = 0, 4, 8, 12, 16, and 20) nano rings:Quantum theory of atoms in molecules/NMR approach. *Journal of Computational and Theoretical Nanoscience* **2014**, *11*, 1290-1298.
39. Monajjemi, M.; Mahdavian, L.; Mollaamin, F.; Honarparvar, B. Thermodynamic investigation of enolketo tautomerism for alcohol sensors based on carbon nanotubes as chemical sensors. *Fullerenes Nanotubes and Carbon Nanostructures* **2010**, *18,* 45-55, https://doi.org/10.1080/15363830903291564.
40. Monajjemi, M.; Ghiasi, R.; Seyed, S.M.A. Metal-stabilized rare tautomers: N4 metalated cytosine (M = Li , Na , K , Rb and Cs), theoretical views. *Applied Organometallic Chemistry* **2003**, *17*, 635-640, https://doi.org/10.1002/aoc.469.
41. Ilkhani, A.R.; Monajjemi, M. The pseudo Jahn-Teller effect of puckering in pentatomic unsaturated rings C AE , A=N, P, As, E=H, F, Cl.*Computational and Theoretical Chemistry* **2015**, *1074*,19-25, http://dx.doi.org/10.1016%2Fj.comptc.2015.10.006.
42. Monajjemi, M. Non-covalent attraction of B N and repulsion of B N in the B N ring: a quantum rotatory due to an external field. *Theoretical Chemistry Accounts* **2015**, *134*, 1-22, https://doi.org/10.1007/s00214-015-1668-9.
43. Monajjemi, M.; Naderi, F.; Mollaamin, F.; Khaleghian, M. Drug design outlook by calculation of second virial coefficient as a nano study. *Journal of the Mexican Chemical Society* **2012**, *56*, 207-211, https://doi.org/10.29356/jmcs.v56i2.323.
44. Monajjemi, M.; Bagheri, S.; Moosavi, M.S. Symmetry breaking of B2N(-,0,+): An aspect of the electric potential and atomic charges. *Molecules* **2015**, *20*, 21636-21657, https://doi.org/10.3390/molecules201219769.
45. Monajjemi, M.; Mohammadian, N.T. S-NICS: An aromaticity criterion for nano molecules. *Journal of Computational and Theoretical Nanoscience* **2015**, *12*, 4895-4914, https://doi.org/10.1166/jctn.2015.4458.
46. Monajjemi, M.; Ketabi, S.; Hashemian, Z.M.; Amiri, A. Simulation of DNA bases in water: Comparison of the Monte Carlo algorithm with molecular mechanics force fields. *Biochemistry (Moscow)* **2006**, *71*, 1-8, https://doi.org/10.1134/s0006297906130013.
47. Monajjemi, M.; Lee, V.S.; Khaleghian, M.; Honarparvar, B.; Mollaamin, F. Theoretical Description of Electromagnetic Nonbonded Interactions of Radical, Cationic, and Anionic NH2BHNBHNH2 Inside of the B18N18 Nanoring. *J. Phys. Chem C* **2010**, *114*, 15315, https://doi.org/10.1021/jp104274z.
48. Monajjemi, M.; Boggs, J.E. A New Generation of BnNn Rings as a Supplement to Boron Nitride Tubes and Cages. *J. Phys. Chem. A* **2013**, *117*, 1670-1684, http://dx.doi.org/10.1021/jp312073q.
49. Monajjemi, M. Non bonded interaction between BnNn (stator) and BN B (rotor) systems: A quantum rotation in IR region. *Chemical Physics* **2013**, *425*, 29-45, https://doi.org/10.1016/j.chemphys.2013.07.014.
50. Monajjemi, M.; Robert, W.J.; Boggs, J.E. NMR contour maps as a new parameter of carboxyl's OH groups in amino acids recognition: A reason of tRNA–amino acid conjugation. *Chemical Physics* **2014**, *433*, 1-11, https://doi.org/10.1016/j.chemphys.2014.01.017.
51. Monajjemi, M. Quantum investigation of non-bonded interaction between the B15N15 ring and BH2NBH2 (radical, cation, and anion) systems: a nano molecularmotor. *Struct Chem* **2012,** *23*, 551–580, http://dx.doi.org/10.1007/s11224-011-9895-8.
52. Monajjemi, M. Metal-doped graphene layers composed with boron nitride–graphene as an insulator: a nano-capacitor.

Journal of Molecular Modeling **2014**, *20*, 2507, https://doi.org/10.1007/s00894-014-2507-y.
53. Monajjemi, M.; Ketabi, S.; Amiri, A. Monte Carlo simulation study of melittin: protein folding and temperature ependence, *Russian journal of physical chemistry* **2006**, *80,* S 55-S62, https://doi.org/10.1134/S0036024406130103.
54. Monajjemi, M; Heshmata, M; Haeria, H.H. QM/MM model study on properties and structure of some antibiotics in gas phase: Comparison of energy and NMR chemical shift. *Biochemistry-moscow* **2006**, *71,* S113-S122 https://doi.org/10.1134/S0006297906130190.
55. Monajjemi, M.; Afsharnezhad, S.; Jaafari, M.R.; Abdolahi, A.N.; Monajemi, H. NMR shielding and a thermodynamic study of the effect of environmental exposure to petrochemical solvent on DPPC, an important component of lung surfactant. *Russian journal of physical chemistry A* **2007**, *81,* 1956-1963, https://doi.org/10.1134/S0036024407120096.
56. Mollaamin, F.; Noei, M.; Monajjemi, M.; Rasoolzadeh, R. Nano theoretical studies of fMet-tRNA structure in protein synthesis of prokaryotes and its comparison with the structure of fAla-tRNA. *African journal of microbiology research* **2011**, *5,* 2667-2674, https://doi.org/10.5897/AJMR11.310.
57. Monajjemi, M.; Heshmat, M.; Haeri, H. H.; et al. Theoretical study of vitamin properties from combined QM-MM methods: Comparison of chemical shifts and energy. *Russian journal of physical chemistry* **2006**, *80,* 1061-1068, https://doi.org/10.1134/S0036024406070119.
58. Monajjemi, M; Chahkandi, B. Theoretical investigation of hydrogen bonding in Watson-Crick, Hoogestein and their reversed and other models: comparison and analysis for configurations of adenine-thymine base pairs in 9 models. *Journal of molecular structure-theochem* **2005**, *714,* 43-60, https://doi.org/10.1016/j.theochem.2004.09.048.
59. Monajjemi, M.; Honarparvar, B.; Haeri, H.H.; Heshmat, M. An ab initio quantum chemical investigation of solvent-induced effect on N-14-NQR parameters of alanine, glycine, valine, and serine using a polarizable continuum model. *Russian journal of physical chemistry* **2006**, *80*, S40-S44, https://doi.org/10.1134/S0036024406130073.
60. Monajjemi, M.; Seyed Hosseini, M. Non Bonded Interaction of $B_{16}N_{16}$ Nano Ring with Copper Cations in Point of Crystal Fields. *Journal of Computational and Theoretical Nanoscience* **2013**, *10*, 2473-2477.
61. Monajjemi, M.; Farahani, N.; Mollaamin, F. Thermodynamic study of solvent effects on nanostructures: phosphatidylserine and phosphatidylinositol membranes. *Physics and chemistry of liquids* **2012**, *50,* 161-172, https://doi.org/10.1080/00319104.2010.527842.
62. Monajjemi, M.; Ahmadianarog, M. Carbon Nanotube as a Deliver for Sulforaphane in Broccoli Vegetable in Point of Nuclear Magnetic Resonance and Natural Bond Orbital Specifications. *Journal of computational and theoretical nanoscience* **2014**, *11,* 1465-1471, https://doi.org/10.1166/jctn.2014.3519.
63. Monajjemi, M.; Ghiasi, R.; Ketabi, S.; Passdar, H.; Mollaamin, F. A Theoretical Study of Metal-Stabilised Rare Tautomers Stability: N4 Metalated Cytosine (M=Be^{2+}, Mg^{2+}, Ca^{2+}, Sr^{2+} and Ba^{2+}) in Gas Phase and Different Solvents. *Journal of Chemical Research* **2004**, *1*, 11-18, https://doi.org/10.3184/030823404323000648.
64. Monajjemi, M.; Baei, M.T.; Mollaamin, F. Quantum mechanics study of hydrogen chemisorptions on nanocluster vanadium surface. *Russian journal of inorganic chemistry* **2008**, *53,* 1430-1437, https://doi.org/10.1134/S0036023608090143.
65. Mollaamin, F.; Baei, M.T.; Monajjemi, M.; Zhiani, R.; Honarparvar, B. A DFT study of hydrogen chemisorption on V (100) surfaces. *Russian Journal of Physical Chemistry A* **2008**, *82,* 2354-2361, https://doi.org/10.1134/S0036024408130323.
66. Monajjemi, M.; Honarparvar, B.; Nasseri, S.M.; Khaleghian, M. NQR and NMR study of hydrogen bonding interactions in anhydrous and monohydrated guanine cluster model: A computational study. *Journal of structural chemistry* **2009**, *50,* 67-77, https://doi.org/10.1007/s10947-009-0009-z.
67. Monajjemi, M.; Aghaie, H.; Naderi, F. Thermodynamic study of interaction of TSPP, CoTsPc, and FeTsPc with calf thymus DNA. *Biochemistry-Moscow* **2007**, *72,* 652-657, https://doi.org/10.1134/S0006297907060089.
68. Monajjemi, M.; Heshmat, M.; Aghaei, H.; Ahmadi, R.; Zare, K. Solvent effect on N-14 NMR shielding of glycine, serine, leucine, and threonine: Comparison between chemical shifts and energy versus dielectric constant. *Bulletin of the chemical society of ethiopia* **2007**, *21*, 111-116, https://doi.org/10.4314/bcse.v21i1.61387.
69. Monajjemi, M.; Rajaeian, E.; Mollaamin, F.; Naderi, F.; Saki, S. Investigation of NMR shielding tensors in 1,3 dipolar cycloadditions: solvents dielectric effect. *Physics and chemistry of liquids* **2008**, *46*, 299-306, https://doi.org/10.1080/00319100601124369.
70. Mollaamin, F.; Varmaghani, Z.; Monajjemi, M. Dielectric effect on thermodynamic properties in vinblastine by DFT/Onsager modelling. *Physics and chemistry of liquids* **2011,** *49,* 318-336, https://doi.org/10.1080/00319100903456121.
71. Monajjemi, M.; Honaparvar, B.; Hadad, B.K.; Ilkhani, A.R.; Mollaamin, F. Thermo-chemical investigation and NBO analysis of some anxileotic as Nano-drugs. *African journal of pharmacy and pharmacology* **2010**, *4,* 521-529.
72. Monajjemi, M.; Khaleghian, M.; Mollaamin, F. Theoretical study of the intermolecular potential energy and second virial coefficient in the mixtures of CH4 and Kr gases: a comparison with experimental data. *Molecular simulation* **2010**, *11,* 865-870, https://doi.org/10.1080/08927022.2010.489557.
73. Monajjemi, M.; Khosravi, M.; Honarparvar, B.; Mollamin, F. Substituent and Solvent Effects on the Structural Bioactivity and Anticancer Characteristic of Catechin as a Bioactive Constituent of Green Tea. *International journal of Quantum Chemistry* **2011**, *111,* 2771-2777, https://doi.org/10.1002/qua.22612.
74. Tahan, A.; Monajjemi, M. Solvent Dielectric Effect and Side Chain Mutation on the Structural Stability of Burkholderia cepacia Lipase Active Site: A Quantum Mechanical/ Molecular Mechanics Study. *Biotheoretica* **2011**, *59*, 291-312, https://doi.org/10.1007/s10441-011-9137-x.
75. Monajjemi, M.; Khaleghian, M. EPR Study of Electronic Structure of [CoF6](3-)and B18N18 Nano Ring Field Effects on Octahedral Complex. *Journal of cluster science* **2011**, *22*, 673-692, https://doi.org/10.1007/s10876-011-0414-2.
76. Monajjemi, M; Mollaamin, F. Molecular Modeling Study of Drug-DNA Combined to Single Walled Carbon Nanotube, *Journal of cluster science* **2012**, *23*, 259-272, https://doi.org/10.1007/s10876-011-0426-y.
77. Mollaamin, F; Monajjemi, M. Fractal Dimension on Carbon Nanotube-Polymer Composite Materials Using Percolation Theory. *Journal of computational and theoretical nanoscience* **2012**, *9*, 597-601, https://doi.org/10.1166/jctn.2012.2067.
78. Mahdavian, L.; Monajjemi, M. Alcohol sensors based on SWNT as chemical sensors: Monte Carlo and Langevin dynamics simulation. *Microelectronics journal* **2010**, *41,* 142-149, https://doi.org/10.1016/j.mejo.2010.01.011.
79. Monajjemi, M.; Falahati, M.; Mollaamin, F. Computational investigation on alcohol nanosensors in combination with carbon nanotube: a Monte Carlo and ab initio simulation. *Ionics* 2013, *19*, 155-164, https://doi.org/10.1007/s11581-012-0708-x.

80. Lu, T.; Chen, F. Multiwfn: A Multifunctional Wavefunction Analyzer. *J. Comp. Chem*. **2012**, *33*, 580-592, https://doi.org/10.1002/jcc.22885.

6. ACKNOWLEDGEMENTS

The author thanks the Islamic Azad university for providing the software and computer equipment.